Atmos. Chem. Phys. Discuss., 14, 23453–23497, 2014
www.atmos-chem-phys-discuss.net/14/23453/2014/
doi:10.5194/acpd-14-23453-2014

Atmospheric Chemistry and Physics Discussions
Open Access

Variability of the mixed phase in the Arctic with a focus on the Svalbard region: a study based on spaceborne active remote sensing

G. Mioche[1], **O. Jourdan**[1], **M. Ceccaldi**[2], **and J. Delanoë**[2]

[1]Laboratoire de Météorologie Physique, Aubière, France
[2]Laboratoire Atmosphères, Milieux, Observations Spatiales, Guyancourt, France

Received: 16 July 2014 – Accepted: 22 August 2014 – Published: 11 September 2014

Correspondence to: O. Jourdan (o.jourdan@opgc.univ-bpclermont.fr)

Published by Copernicus Publications on behalf of the European Geosciences Union.

Abstract

The Arctic region is known to be very sensitive to climate change. Clouds and in particular mixed phase clouds (MPC) remain one of the greatest sources of uncertainties in the modeling of the Arctic response to climate change due to an inaccurate representation of their variability and their quantification. In this study, we present a characterization of the vertical, spatial and seasonal variability of Arctic clouds and MPC over the whole Arctic region based on satellite active remote sensing observations. MPC properties in the region of Svalbard archipelago (78° N, 15° E) are also investigated. The occurrence frequency of clouds and MPC are determined from CALIPSO/CLOUDSAT measurements processed with the DARDAR retrieval algorithm which allows for a reliable cloud thermodynamic phase classification (warm liquid, supercooled liquid, ice, mixing of ice and supercooled liquid). Significant differences are observed between MPC variability over the whole Arctic region and over the Svalbard region. Results show that MPC are ubiquitous all along the year, with a minimum occurrence of 30 % in winter and 50 % during the rest of the year, in average over the whole Arctic. Over the Svalbard region, MPC occurrence is more constant with time with larger values (55 %) compared to the average observed in the Arctic. MPC are especially located at low altitudes, below 3000 m, where their frequency of occurrence reaches 90 %, in particular during winter, spring and autumn. Moreover, results highlight that MPC statistically prevail over sea. The temporal and spatial distribution of MPC over the Svalbard region seems to be linked to the contribution of moister air and warmer water from the North Atlantic Ocean which contribute to the initiation of the liquid water phase. Over the whole Arctic, and particularly in western regions, the increase of MPC occurrence from spring to autumn could be connected to the sea ice melting. During this period, the open water transports a part of the warm water from the Svalbard region to the rest of the Arctic region. This facilitates the vertical transfer of moisture and thus the persistence of the liquid phase. A particular attention is also paid on the measurements uncertainties and how they could affect our results.

ACPD
14, 23453–23497, 2014

1 Introduction

It is now well established that the Arctic region is more sensitive to climate change than any other regions of the world (Sanderson et al., 2011; Serreze et al., 2009; Solomon et al., 2007). Solar elevation or surface albedo for instance are responsible for strong feedback mechanisms leading to the so-called Arctic amplification. Clouds are one of the main components driving the Arctic climate system as they play a key role in the radiation budget (Curry, 1995; Curry et al., 1996; Garrett et al., 2009). They cool or warm the surface and the atmosphere depending on their macrophysical and microphysical properties which control their interactions with shortwave and longwave radiation. In particular, the low sun elevation in summer and the lack of solar radiation during the winter polar night cause a dominance of the longwave radiative effect in the Arctic, tending to a global net warming effect.

However, our sparse knowledge of cloud-radiation interactions and cloud properties at high latitudes remains one of the main source of uncertainties in predicting future climate by numerical simulations (Solomon et al., 2007; Stephens, 2005). In particular, the determination of cloud thermodynamic phase is crucial for assessing the cloud radiative impact and hence, its influence on the radiation budget and climate feedbacks (Choi et al., 2014; Komurcu et al., 2014).

The Arctic is precisely known for the frequent occurrence of mixed phase clouds (hereafter MPC) especially near the surface, wherein liquid droplets and ice crystals coexist (Curry et al., 2000; Korolev and Isaac, 2003; Shupe, 2011). Moreover, because these clouds often occur near the ground, their radiative interaction with the bright surface is strong. Nevertheless, even though MPC have been studied for years from numerous observations, as well as numerical modeling (Verlinde et al., 2007; de Boer et al., 2009; Gayet et al., 2009; Jourdan et al., 2010; McFarquhar et al., 2011, among others), results still suffer from large uncertainties and important discrepancies are observed between observations and simulations (Chernokulsky and Mokhov, 2012; Klein et al., 2009; Morrison et al., 2009; Thomas et al., 2004).

ACPD
14, 23453–23497, 2014

Previous studies based on observations or modeling, highlighted that the various steps of MPC life cycle such as formation, development, persistence or dissipation, are due to the combination of local and large-scale processes. For example, at small scale, the Wegener–Bergeron–Findeisen mechanism is one of the main microphysical processes responsible for ice crystals growth at the expense of supercooled water droplets (Bergeron, 1935; Findeisen, 1938; Wegener, 1911). Such a mechanism tends to rapidly cause the entire glaciation of MPC. Nevertheless, additional dynamical processes, such as turbulence or entrainment, (Morrison et al., 2012) resupply of water vapor from the surface and from entrainment of moisture from above the clouds facilitate the persistence of supercooled water droplets. The coupling of such various processes is thus necessary to maintain the unstable equilibrium between liquid droplets and ice crystals within MPC. Thereby, the combination of these various processes at different scales can explain the longevity of MPC up to several days or weeks as it has been frequently observed (Shupe, 2011; Verlinde et al., 2007; Morrison et al., 2012). Peculiar meteorological conditions, as well as local and long-range dynamic processes are also involved during aerosols, heat and moisture transport which have a significant impact on Arctic MPC formation and properties (Cesana et al., 2012; Morrison et al., 2012; Shupe and Intrieri, 2004). However, the macrophysical and microphysical characterization of MPC on the whole Arctic region, as well as their spatial and temporal variability, is not yet accurately described. Therefore it is difficult to fully understand the complexity of interactions between all these processes and assert which of them play a key role in MPC evolution (Harrington et al., 1999; Morrison et al., 2012).

The characterization of the Arctic cloud mixed phase state at global and local scales is particularly challenging due to remote and extreme conditions encountered in this region of the world. For these reasons observations remain very sparse. Ice crystals and liquid droplets exhibit significantly different microphysical and optical properties (number, size, shape), leading to different interactions with radiation. The impact of the mixed phase on the energy budget and climate is thus strongly dependent on the ice/liquid partitioning. Moreover, the discrimination of ice crystals and liquid droplets

ACPD
14, 23453–23497, 2014

remains challenging due to instrument limitations in both remote sensing and in-situ measurements (Baumgardner et al., 2012).

Multi and single-layer clouds are the two main MPC types frequently observed in the Arctic. Multilayer MPC consist of several supercooled liquid layers embedded in ice clouds at different altitude levels. Ice crystals precipitate from upper layers feeding underneath layers or evaporating during sedimentation, leading to very complex interactions between ice crystals and droplets (Hobbs and Rangno, 1998; Luo et al., 2008).

On the other hand, the typical single-layer MPC structure is characterized by the presence of a unique supercooled liquid layer at cloud top and ice crystals below, precipitating down to the surface (Curry et al., 1997; Shupe et al., 2005; Verlinde et al., 2007; Gayet et al., 2009). This peculiar vertical structure has been frequently observed at small scale in previous airborne experiments such as the Arctic Study of Tropospheric cloud, Aerosol and Radiation (ASTAR, Gayet et al., 2009; Jourdan et al., 2010) in 2004 and 2007, the Polar Study using Aircraft, Remote Sensing Surface Measurements and Models of Climate, Chemistry, Aerosols and Transport (POLARCAT, Delanoë et al., 2013) in 2008, the Indirect and Semi-Direct Aerosol Campaign (ISDAC, McFarquhar et al., 2011) in 2008 or the Solar Radiation and Phase Discrimination of Arctic Clouds (SORPIC, Bierwirth et al., 2013) in 2010 (Ehrlich et al., 2009; Gayet et al., 2009; Jackson et al., 2012; McFarquhar et al., 2007). However, this structure is not yet completely understood, and its impact on the radiation budget must be determined with a better accuracy (Klein et al., 2009; Morrison et al., 2009). Moreover, an assessment of the representativity of in situ measurements, which are by essence localized in time and space, is needed. So, a description of Arctic MPC at regional scale is first necessary.

Although clouds measurements still remain challenging in this region, important progresses have been made for several years. In particular, several ground-based observation sites are now well equipped for cloud observations, such as Barrow (71° N), Eureka (80° N), Summit (72° N) or Ny-Alesund (78° N) observatories. However, the instruments of each ground observatory may differ significantly from one site to another. Indeed, climatologies based on different instruments can be biased by the sensitivity of the instruments and their capability to operate in extreme conditions. For instance it is very difficult to compare results derived from a lidar and from a cloud radar as they will not be sensitive to the same hydrometeors. During the last decade the emergence of spaceborne observation platforms provide a large amount of cloud related data (AVHRR, ISCCP, MODIS, A-Train). Unlike ground-based sites, they present the great advantage to involve a uniform measurement technique with a very large coverage (almost the entire Arctic region). In particular the new generation of spaceborne instrumentation onboard CALIPSO (Winker et al., 2003) and CloudSat (Stephens et al., 2002) satellites (active remote sensing formed by of 532 and 1064 nm lidar and 94 GHz radar) provide since 2006 an unprecedented dataset of the vertical structure of clouds, continuously in time and space.

The aim of this study is to characterize the vertical, spatial and seasonal variability of Arctic MPC at regional scale from space remote sensing. A focus on MPC properties in the area around the Svalbard archipelago (78° N, 15° E), which benefits from distinctive meteorological conditions due to the proximity of North Atlantic Ocean compared to the rest of Arctic, will also be performed. This will enable us to evaluate to which extent MPC in this region are representative of their counterparts over the whole Arctic. In addition, this work will give an insight into the representativity of the numerous airborne cloud measurements made in this region for several years (ASTAR, POLARCAT, SORPIC among others).

This work is based on the radar-lidar spaceborne measurements synergy with CloudSat/CALIPSO observations. Cloud thermodynamic phase and distribution are determined from DARDAR retrieval products (Delanoë and Hogan, 2008, 2010 and recently Ceccaldi et al., 2013). Then properties over the Svalbard region are investigated and compared to those at regional scale. Section 2 describes the DARDAR retrieval algorithm and presents the dataset used and the method applied to detect MPC and determine cloud occurrences. In Sect. 3, total cloud occurrence determined from DARDAR products is first compared to previous works in order to validate the methodology. Then in Sect. 4, focus is made on mixed-phase clouds variability at global scale and over the region of Svalbard. In Sect. 5, global and local MPC properties are compared and differences observed between the whole Arctic and the Svalbard region are discussed.

2 Data and method

Cloud thermodynamic phase distributions over the Arctic region are studied using CALIPSO and CloudSat measurements. Active remote sensing observations are expected to provide a detailed characterization of the cloud vertical structure in the Arctic. Indeed, compared to passive instruments, active remote sensing is less disturbed by the important Arctic ice cover throughout the year or the lack of sunlight during the polar night (Chan and Comiso, 2013; Liu et al., 2010; Wang and Key, 2005).

2.1 DARDAR retrieval algorithm

The present study is based on the operational DARDAR (for raDAR/liDAR) retrieval products. DARDAR algorithm (Delanoë and Hogan, 2008, 2010) exploits the synergy of CALIPSO and CloudSat observations to determine cloud thermodynamic phase (DARDAR-MASK product) and to retrieve ice cloud properties (DARDAR-CLOUD product). These products are now widely used for the cloud studies (Delanoë et al., 2013; Huang et al., 2012; Jouan et al., 2012, 2014). DARDAR-MASK algorithm uses collocated Level 1B CALIPSO 532 nm lidar backscatter coefficient profiles, "2B-GEOPROF" CLOUDSAT 94 GHz radar reflectivity as well as thermodynamic variables (pressure, temperature, humidity) from "ECMWF-AUX" products on a 60 m vertical and 1 km horizontal resolution grid. The combination of both LIDAR and RADAR cloud masks is then used to classify cloud hydrometeors phase. The main steps of the algorithm for cloud thermodynamic phase retrieval are summarized in Fig. 1 and all DARDAR retrieval classes are summarized in Table 1. This includes surface and clear sky detection (class

Discussion Paper | Discussion Paper | Discussion Paper | Discussion Paper |

ACPD

14, 23453–23497, 2014

Variability of the mixed phase in the Arctic with a focus on the Svalbard region

G. Mioche et al.

−1 and 0 respectively), cloudy pixels with ice only (class 1), mixing of ice and supercooled water (class 2), cloud warm liquid (class 3), supercooled liquid (class 4), rain (class 5) as well as stratospheric features (class 8), and aerosols and insects detection (class 6 and 7 respectively). In particular, a cloud layer is classified as supercooled water if its lidar backscatter signal, β, is higher than $2.10^{-5}\,\mathrm{m^{-1}\,sr^{-1}}$ and if it strongly (at least 10 times) and rapidly (in the next 480 m) attenuates the lidar signal. Note that the lidar is very sensitive to small drops in high concentration and therefore the backscattered signal, in presence of liquid drops, is very high and a strong attenuation is expected below the backscattering peak. Moreover, to be classified as supercooled water, a cloud layer needs to be located in the temperature range from 0 to −40 °C (temperature of homogenous nucleation) and to have a physical thickness (detected by the lidar) thinner than 300 m. When supercooled water is detected, confident detection of cloud features by radar (i.e. when CloudSat cloud mask values are greater than 30) determines if ice is present or not in the same sample volume. All cloud features with a temperature less than −40 °C are considered as ice. One can note that this retrieval technic only works when the lidar is operational.

A complete description of DARDAR algorithm is presented in Delanoë and Hogan (2008, 2010) and reminded in Ceccaldi et al. (2013). Version 1 of DARDAR-MASK (v.1.1.4), distributed by the French data center ICARE, is used in this study and provides a categorization of pixels according to the classes summarized in Table 1.

2.2 Dataset and methodology

First, it is necessary to precise the definition of mixed phase clouds used in the present study. All DARDAR pixels classified as mixing of ice and supercooled water (class 2, see Table 1) or all pixels classified as supercooled only (class 4, see Table 1) associated with the presence of ice or ice and supercooled water mixing in the vicinity of the pixel are assumed to belong to the mixed phase class (or are considered as mixed phase pixels). “Isolated” supercooled water pixels are not classified as mixed phase clouds.

The annual and seasonal variability of total cloud fraction and MPC is investigated using CALIPSO/CloudSat continuous measurements from 2007 to 2010. In this study the Arctic region is defined by all latitudes greater than 60° N (Liu et al., 2012) and the Svalbard region is defined as the area between 0 and 30° E of longitude and 75 and 80° N of latitude.

The Spatial frequency of occurrence and vertical distributions are determined for both total cloud and MPC. The spatial distribution of clouds is studied for altitudes spanning from 500 m up to 12 km, according to the study of Liu et al. (2012) as well as for low-level altitude ranging between 500 m and 3 km (according to Zygmuntowska et al., 2012). A minimum altitude of 500 m is chosen to avoid surface contamination in CloudSat data (Marchand et al., 2008) and also to prevent from false water detection (due to the lidar high backscattered signal from the ground) in DARDAR algorithm. These instrument shortcomings will be discussed further in Sect. 5. The seasonal occurrence is calculated taking into account March-April-May (MAM) for spring, June-July-August (JJA) for summer, September-October-November (SON) for fall and December-January-February (DJF) for winter. The horizontal spatial resolution of cloud occurrence is 5° in longitude and 2° in latitude and the vertical resolution is 60 m for the profiles.

For each season (or month), cloud and MPC spatial occurrences (hereafter F_{CLOUD} and F_{MPC}) in each box of 2° latitude by 5° longitude (Δlat, Δlon) are computed as followed:

$$F_{\mathrm{CLOUD}}(\Delta\mathrm{lat},\Delta\mathrm{lon}) = \frac{\sum_{i,j} N_{\mathrm{CLOUD}}(i,j)}{N_{\mathrm{footprints}}} \tag{1}$$

$$F_{\mathrm{MPC}}(\Delta\mathrm{lat},\Delta\mathrm{lon}) = \frac{\sum_{i,j} N_{\mathrm{MPC}}(i,j)}{\sum_{\mathrm{i,\,j}} N_{\mathrm{CLOUD}}(i,j)} \tag{2}$$

ACPD
14, 23453–23497, 2014

where (i, j) are the latitudes and longitudes of the CALIPSO/CLOUDSAT granules falling into the 2° latitude by 5° longitude box (Δlat width by Δlon length).

$N_{\text{footprints}}$ is the total number of footprints in the 2° latitude by 5° longitude box.

$N_{\text{CLOUD}}(i,j)$ (and $N_{\text{MPC}}(i,j)$) is the occurrence of clouds (and MPC) in the atmospheric column at latitude i and longitude j, and is defined as follow:

$$\begin{aligned} N_{\text{CLOUD or MPC}}(i,j) &= 1 \quad \text{if} \sum_{z_{\min}}^{z_{\max}} n_{\text{CLOUD or MPC}}(i,j,z) \geq 3 \\ &= 0 \quad \text{if} \sum_{z_{\min}}^{z_{\max}} n_{\text{CLOUD or MPC}}(i,j,z) < 3 \end{aligned} \tag{3}$$

where $z_{\min}$ and $z_{\max}$ are the altitude boundaries for occurrence calculation. $z_{\min}$ = 500 m and $z_{\max}$ = 12 km or 3 km depending on the altitude range taken into account (all-level or low-level domain respectively).

$n_{\text{CLOUD}}(i,j,z)$ (and $n_{\text{MPC}}(i,j,z)$) refers to the detection of clouds (and MPC) at altitude z and coordinates (i, j). It is equal to 1 if cloud (or MPC) is present, and 0 if not.

So, the presence of cloud (and MPC) is detected in each atmospheric column if at least 3 pixels are classified as cloud (MPC) by DARDAR.

The vertical distribution of MPC occurrence (hereafter $F_{\text{MPC}}(z)$) is computed at each altitude level z according to the following equation:

$$F_{\text{MPC}}(z) = \frac{\sum_{i,j} N_{\text{MPC}}(i,j,z)}{\sum_{i,j} N_{\text{CLOUD}}(i,j,z)} \tag{4}$$

where i and j are the latitudes and longitudes of the CALIPSO/CLOUDSAT granules falling into the considered domain, i.e. the Svalbard region (75–80° N, 0–30° E) or the whole Arctic region (area above 60° N).

ACPD
14, 23453–23497, 2014

It should be also noted that the term "CLOUD" used in Eqs. (2) and (3) refers to clouds at temperatures colder than 0 °C. Warm clouds ($T > 0$ °C) are not considered in the determination of MPC occurrence.

3 Total cloud occurrence (F_{CLOUD})

Arctic total cloud occurrence (F_{CLOUD}) and its annual variability have been already extensively studied. Most of the previous studies are based on passive remote sensing observations performed by instruments such as AVHRR, CERES, ISCCP, MODIS (Frey et al., 2008; Key and Barry, 1989; Rossow and Garder, 1993; Wielicki et al., 1996). However, the limitations of these observations in this region of the world are now well-known. Comparing ground based observations with ISCCP and Nimbus-7 passive remote sensing spaceborne platforms, Schweiger and Key (1992) showed for example that the satellite derived cloud fraction is generally smaller than the surface observations by 5–35 %. More recently, Liu et al. (2010) highlighted that the low contrast between clouds and the underlying surface in nighttime conditions can lead to an underestimation of the cloud amount from MODIS observations by 20 %, compared to CALIPSO-CloudSat. Chan and Comiso (2013) found that clouds not detected by MODIS were mainly localized above 6 km and below 2 km.

Active remote sensing technique can overcome these limitations. Nowadays, several ground based observations sites are well-equipped with such instrumentation (Barrow, Eureka, NyAlesund, Summit). However these observations remain localized in space and measurement techniques could vary from one site to another. Thus, the inhomogeneity and the representativity of these Arctic ground-based observations could be an issue.

Figure 2a shows the monthly total cloud occurrence F_{CLOUD} over the Arctic region derived from DARDAR along with an overview of the main past studies. F_{CLOUD} obtained at the main observation sites and from main past experiments are reported (namely Atqasuk, Barrow, Eureka, the Surface Heat Budget of the Arctic Ocean experiment

ACPD
14, 23453–23497, 2014

(SHEBA), summarized in Orbaek et al. (1999), Dong et al. (2010) and Shupe et al. (2011) works, as well as the standard NASA CALIPSO-CloudSat products for 2007 and 2008 (Zygmuntowska et al., 2012). Figure 2b focuses on the Svalbard region and reports the monthly F_{CLOUD} determined from DARDAR products along with visual and MPL ground based observations in Ny-Alesund and ISCCP measurements (Orbaek et al., 1999; Shupe et al., 2011).

The large differences observed in Fig. 2a between ground based and spaceborne measurements could be partly explained by the ability of ground observatories to more accurately detect low-level clouds (Blanchard et al., 2014). However, the variability within ground based measurements remains significant due to the discrepancies of the measurement technics or the localization of the observatories. Furthermore, comparing the annual or seasonal variability over western Arctic regions (Fig. 2a) and over the Svalbard region (Fig. 2b), no noticeable trend is observed: on Fig. 2b, Ny-Alesund ground visual and MPL observations show a maximum occurrence in summer and early autumn (~ 70–80 %), while ISCCP observations indicate an opposite trend over the ocean on the west side of Svalbard. Moreover, in western Arctic (SHEBA experiment and Eureka, Barrow and Atqasuk sites on Fig. 2a), cloud variability is significantly different: maximum cloud occurrence values are observed in spring and mostly in autumn, ranging from 80 to nearly 100 %.

These discrepancies highlight the need for global observations with a uniform measurement technique. This requirement is fulfilled with spaceborne observations, in particular those provided by CloudSat and CALIPSO. Standard NASA retrieval products from CALIPSO-CloudSat in 2007 and 2008 (2B-GEOPROF-LIDAR products, Zygmuntowska et al., 2012) as well as DARDAR products are reported on Fig. 2a. Both products show an annual variability with two maxima in spring and autumn. As expected, NASA and DARDAR products are consistent, justifying the methodology based on DARDAR products proposed for this study. Small differences in the two products could result from the data processing methodology (differences linked to the geographical domain of the studied area and surface type taken into account, vertical resolution

ACPD
14, 23453–23497, 2014

difference between NASA and DARDAR products). On Fig. 2b, annual variability of cloud occurrence from active and passive space remote sensing observations (A-Train and ISCCP) are not well consistent with Ny-Alesund ground based measurements. Ground based observations show a maximum occurrence during summer (between 60 and 80 %), while spaceborne observations show a minimum in that season. However, annual variability from DARDAR may be considered as consistent with that from ISCCP over the same area i.e. over ocean on the west cost of Svalbard, even if ISCCP observations seem to show a notable and expected underestimation.

Finally, when comparing F_{CLOUD} over the whole Arctic and over the Svalbard region from Fig. 2a and b, one can note that, apart from summer, Svalbard region presents all along the year a total cloud occurrence larger than the mean Arctic occurrence by at least 5 %. Especially in winter and spring, cloud occurrence over Svalbard is larger than the Arctic average by about 20 %.

4 Mixed phase clouds and single layer mixed phase clouds occurrence

4.1 Mixed phase clouds (F_{MPC})

Among all clouds, it is well established that mixed phase clouds (MPC) commonly occur in the Arctic (Curry et al., 1996; Shupe et al., 2006; Verlinde et al., 2007). In particular, low-level MPC are prevalent and exert a large influence on the surface radiation budget, as shown in the study of Shupe and Intrieri (2004) based on ground based measurements during the SHEBA experiment (Uttal et al., 2002). However, the inter annual spatial variability of Arctic MPC properties has been poorly quantified at a large scale due to the lack of observations. An assessment of the annual variability of MPC was performed during SHEBA, showing that mixed phase clouds and liquid-containing clouds are prevalent over Barrow, Alaska. SHEBA experiment highlighted that liquid containing clouds (i.e. including warm liquid cloud) occurrence over the Beaufort sea is at least 40 % (in winter) and reaches more than 90 % (in summer), according to Intrieri

ACPD
14, 23453–23497, 2014

et al. (2002). Mixed phase cloud occurrence is between 20 and 50 %, according to Curry et al. (1996), Shupe et al. (2006) or Verlinde et al. (2007).

The stereographic projection of the mean seasonal arctic F_{MPC} is displayed in Fig. 3a, together with timeseries of monthly F_{MPC} (Fig. 3b). F_{MPC} is determined for an altitude domain between 500 m and 12 km. One can note that MPC are ubiquitous in all seasons almost anywhere in the Arctic region. They seem to be linked to the surface type as larger occurrences are observed over ocean than over land, espacially in the Greenland Sea and Barents Sea region. In particular from May to October, nearly 50 % of the clouds over the whole arctic region are MPC, (top panel of Fig. 3b). In winter and early spring, F_{MPC} is close to 30 %. However, the spatial and temporal distribution of MPC is highly inhomogeneous. Larger occurrences up to 60 % are observed over the Greenland Sea throughout the year and over the Canadian basin and the Chukchi Sea in fall. Over the Svalbard region (Fig. 3b, bottom panel), F_{MPC} is larger compared to the Arctic average, and less contrasted, with values around 55 %, ranging between 45 and 60 % all year long.

Figure 4a presents the vertical profiles of the mean seasonal vertical distribution (F_{MPC} (z)), over the whole Arctic and over the Svalbard region. Figure 4b displays the mean seasonal F_{MPC} computed from Eqs. (1)–(3), according to the ground type (land and sea surfaces) obtained from the land/water mask available in DARDAR product. Note that sea surface includes both open water and sea ice. The grey zone on each profile in Fig. 4a represents the region below 500 m, where space remote sensing data are considered not reliable because of the surface contamination. For altitude below 3000 m, F_{MPC} (z) sharply increases with decreasing altitude at the exception of summer observations. During the transition seasons (spring and fall), the maximum occurrence of MPC is reached between 500 m and 1500 m a.s.l. with values higher than 15 and 20 % over the whole Arctic and over the Svalbard region respectively. Above a typical altitude of 3000 m, the MPC frequencies decrease below 10 %. The main result stemming from these figures is that MPC prevail mainly at low altitudes lower than 3000 m both over the whole Arctic and over the Svalbard region. The largest

ACPD
14, 23453–23497, 2014

occurrences are observed below this altitude level with values almost twice as large as the one encountered above. F_{MPC} (z) in both regions exhibit similar characteristics despite a more pronounced low level cloud increase over the Svalbard region. However, in summer, the vertical profile F_{MPC} (z) is characterized by a higher cloud amount above 3000 m and less cloud below 3000 m.

Figure 4b highlights that MPC are more present over sea than over land. This difference is rather small over the whole Arctic, but more pronounced in the Svalbard region (except in summer where no difference is observed). In particular during winter and spring, MPC are more present over ocean than over land by up to 20 %. This result is consistent with the spatial variability displayed on Fig. 3a. Moreover, results for all-level altitude domain (500 m to 12 km, Fig. 4b top panel) and for low-level domain (500 m to 3 km, Fig. 4b bottom panel) are very similar. Only the summer present significant higher values for the all-level altitude domain.

Figure 5a and b display respectively the monthly low-level F_{MPC} as well as the ratio of low-level MPC over total MPC. Monthly low-level F_{MPC} is clearly characterized by two peaks in spring and autumn, and a clear decrease in summer. Figures 3b and 5a and b, highlight that MPC clouds are mostly confined at low altitudes, except in summer. Figure 5b shows that nearly 70 and 90 % of the MPC (over the Arctic region and the Svalbard region respectively) are located below 3000 m. Summer season presents a large decrease of this ratio, with values down to 30 % for the whole Arctic and 40 % for the Svalbard region. In summer, low level MPC are less frequent (30 %) which is consistent with the vertical profiles displayed on Fig. 4a showing a significant occurrence of MPC in the mid-level altitude domain (3000–6000 m). Finally, Fig. 5b highlights that the fraction of low level MPC in the Svalbard region is systematically higher than the Arctic average (10 to 20 % more, mainly in winter and spring).

4.2 Single layer mixed phase clouds ($F_{MPC\text{-}IB}$)

Finally, we determine the occurrence of a specific type of Arctic MPC: single layer mixed phase clouds characterized by supercooled liquid at the top and ice below, precipitating down to the surface. This type of cloud will be noted thereafter MPC-IB (for Mixed-Phase Cloud with Ice Below). In DARDAR products, pixels identified as mixed-phase and presenting at least 3 ice pixels below them are classified as MPC-IB type. Clouds characterized by ice pixels above a liquid layer (i.e. corresponding to an embedded mixed-phase) are rejected.

First, we estimate the proportion of MPC-IB among MPC. Figure 6 displays the ratio of MPC-IB over MPC for the low-altitude domain (500 m–3 km), both for the whole Arctic and the Svalbard region. The variability of this ratio is rather small throughout the year. The proportion of MPC-IB among MPC varies between 55 and 70 % over the whole Arctic and between 65 and 80 % over the Svalbard region.

As it was made for MPC, the main characteristics of the MPC-IB occurrences are also studied. They are displayed on Figs. 7 and 8 in a similar matter as Figs. 4 and 5. From these figures, it is noteworthy that vertical distribution and seasonal variability of MPC-IB clouds are very similar to those of MPC, with values generally smaller by around 10–15 % compared to MPC. Indeed, except in summer, MPC-IB are mainly present at low-level altitudes (Fig. 7a), both for the whole Arctic and the Svalbard region. MPC-IB are preferentially located over ocean (Fig. 7b). This trend is observed both over the whole Arctic and the Svalbard region. However, this feature is very pronounced during spring in the Svalbard region where the MPC-IB occurrence over the sea is almost two times higher than over land, as well as during autumn for the whole Arctic.

The annual variability displayed on Fig. 8a shows that MPC-IB are mainly present in spring and fall on the whole Arctic (with respectively occurrences around 25 and 30 %). The Svalbard area presents larger $F_{\text{MPC-IB}}$ than the whole Arctic by around 5–10 %. At last, the ratio of low-level MPC-IB over total MPC-IB, displayed in Fig. 8b, highlights that low-level MPC-IB represent up to 60 and 80 % of the MPC-IB, over the whole Arctic and over the Svalbard region respectively. Only the summer season is characterized by a strong decrease of this ratio, when their presence in upper levels is significant, as it was the case for MPC (Fig. 5b).

ACPD
14, 23453–23497, 2014

At global and regional scales, MPC-IB characteristics over the Arctic region and over the Svalbard region are thus very similar to those of MPC: they are ubiquitous all along the year, more present over ocean than land, and more present in the Svalbard region, particularly in spring.

5 Discussion

5.1 Uncertainties in the climatology

In the previous section, a climatology of the MPC occurrence based on CALIPSO/CLOUDSAT observations is performed. However we first have to keep in mind that space remote sensing measurements and retrieval products suffer from some uncertainties, due to the measurement technique and the retrieval method. We propose to look at them in the first part of this discussion and estimate how they could impact the results of the present study.

First, space remote sensing presents inherent and well-known shortcomings near the ground. For example, CloudSat radar ground echoes lead to an overestimation of low-level cloud amount (Marchand et al., 2008) if the radar clutter is not properly removed. On the other hand, the probability of total or partial attenuation of lidar laser beam by upper cloud layer increases when approaching ground level and could induce an underestimation of the cloud amount assessed by the lidar. The difficulty for DARDAR algorithm to distinguish ground lidar attenuated backscattering signal from an overlaying liquid layer is another shortcoming in the retrieval method, which can lead to a cloud misclassification. The final impact (overestimation or underestimation) of these different issues on low-level cloud occurrence remains uncertain.

To minimize these uncertainties, a minimum altitude threshold of 500 is chosen in the present study to compute cloud occurrence. (We recall here that the original CloudSat vertical resolution is 240 m, so this threshold corresponds to two CloudSat pixels.) Data below this altitude threshold present a non-realistic and very large variability, as shown

ACPD
14, 23453–23497, 2014

on vertical profiles in Fig. 4a. Moreover, ground contamination could also affect Cloudsat cloud detection measurements above an altitude of 500 m. For example, Kay and Gettelman (2009) used a detection altitude limit of 720 m to prevent false detection. On the other hand, Huang et al. (2012) showed that DARDAR data between 700 and 1000 m were reliable for cloud occurrence determination. In the present study, a short sensitivity test is made by computing cloud occurrences with a threshold of 1000 m in order to check differences with occurrence with a 500 m altitude threshold. When considering a 1000 m threshold, the occurrence results are smaller than those obtained with a 500 m threshold. Differences lie between 4 and 18 % depending on the cloud type and the altitude domain considered, as presented in Fig. 9. These results are consistent with similar tests made on CALISPO/CloudSat standard NASA products by Zygmuntowska et al. (2012) showing that F_{CLOUD} derived with a 1000 m minimum altitude threshold is smaller than the F_{CLOUD} derived with a 500 m minimum altitude threshold by up to 26 %. However, while it is well established that cloud amount below 500 m is inaccurate due to ground echoes contamination, it can be reasonable to think that such ground echoes have less influence in the 500 to 1000 m altitude range. In this altitude domain, cloud detection is probably predominant compared to false detection due to ground echoes. For this reason, and reminding that the goal of this work is the study of clouds and MPC in particular at low altitudes, we keep a minimum altitude threshold of 500 m.

One more ambiguity concerning MPC, and in particular MPC-IB, is the ability of the remote sensing to detect several liquid layers. Indeed, the lidar suffers from a strong attenuation when liquid is present and therefore it is very difficult to detect more than one supercooled liquid layer. Therefore, the detection of multi-layer MPC from remote sensing may be hampered, inducing an inaccurate classification of multi-layer MPC in MPC-IB, and thus a possible overestimation of the occurrence of MPC-IB.

An additional shortcoming concerns the DARDAR retrieval algorithm. DARDAR detects supercooled liquid (and warm liquid) layers from a strong lidar backscatter signal (see Fig. 1). But some additional pixels with a strong backscatter signal located above

ACPD
14, 23453–23497, 2014

and below the liquid layer can also be misclassified as liquid. So, these additional supercooled pixels may lead to an overestimation of supercooled liquid water occurrence and supercooled liquid layers thickness. The present study uses version 1 of DARDAR products, but a second version has been developed since this work, including upgraded processing method (Ceccaldi et al., 2013) and will be distributed in the future by ICARE. In particular, this new version removes these additional pixels which are included by the version 1 of DARDAR algorithm. The detailed study by Ceccaldi et al. (2013) showed that globally ice fraction increases by a factor of about 15 % in version 2, associated to a decrease of supercooled water fraction (up to 25 %), compared to version 1. Therefore, version 1 may overestimate supercooled liquid layers thickness, and thus the occurrence of mixed phase clouds too. In order to quantify how these differences can affect the results of the present study, comparisons are performed between the two products versions over one month of data (April 2007). Figure 10a shows differences between the two versions in terms of F_{CLOUD}, F_{MPC} and $F_{\mathrm{MPC\text{-}IB}}$ for the low-level and the all-level altitude domains. Differences are between 3 and 15 % for the whole Arctic, and between −2 and 8 % on the Svalbard region. Finally, Fig. 10b presents the mean vertical profiles extracted from both data versions. The trends are similar but V2 present smaller values for clouds and MPC by about 5 %. Only ice phase is larger with V2, by around 5–10 %. One can also note that on Fig. 10b F_{MPC} with V2 presents an anomalous large peak below 500 m. The reason is that in V2, F_{CLOUD} is very small below 500 m, compared to V1, because of a larger proportion of pixels identified as "unknown", or "multiple scattering due to supercooled water".

At last, as shown in Fig. 1, supercooled and mixed phase pixel detection from DARDAR algorithm is dependent on the a priori threshold considered for variables such as temperature or layer thickness. In particular, temperature is determined based on ECMWF reanalysis, and its accuracy may be a source of error in supercooled liquid retrieval algorithm. However, the ECMWF temperature uncertainty is estimated to 0.6 K (Benedetti, 2005) which is considered as acceptable by Delanoë and Hogan (2010).

ACPD
14, 23453–23497, 2014

Title Page
Abstract | Introduction
Conclusions | References
Tables | Figures
◂◂ | ▸▸
◂ | ▸
Back | Close
Full Screen / Esc
Printer-friendly Version
Interactive Discussion

In this study, the Arctic region is considered northward 60° N as it is made in several previous studies (Cesana et al., 2012; Chernokulsky and Mokhov, 2012; Liu et al., 2012 among others). However, no real definition of Arctic region is truly established, and some authors used a different limit, such as 65° N (Kay and Gettelman, 2009; Nygård et al., 2014), 68° N (Zygmuntowska et al., 2012) or 70° N (de Boer et al., 2012). These latitude boundaries were tested (not shown here) and differences observed on clouds and MPC occurrences are not significant since they vary only by a few % (by less than 5 % between 60 and 70° N limits).

5.2 Total cloud and MPC variability

Keeping in mind these main uncertainties and precisions, we show that on the Arctic global scale, total cloud occurrence computed from DARDAR products is, as expected, consistent with NASA standard products. Concerning the Svalbard region, total cloud occurrence exhibits larger values (up to 20 % larger) than the Arctic average, all along the year, especially in winter and spring. The investigation of MPC occurrence highlights that total MPC are ubiquitous throughout the year in the Arctic and more specifically over the Svalbard region. Annual variability shows a large presence of MPC from May to October over the whole Arctic (50 %), associated with a minimum in winter (30 %), while MPC are rather constant throughout the year over Svalbard (around 50 %). Moreover, MPC and typical MPC made by supercooled liquid at cloud top and ice below (MPC-IB) prevail at low altitudes (< 3000 m). MPC and MPC-IB occurrence in this altitude domain represent up to 90 and 80 % of the total amount of MPC and MPC-IB, respectively. Their annual variability is characterized by two maxima in spring and autumn. During spring, MPC and MPC-IB are located mainly over the Greenland, Barents and Norwegian seas. In autumn, large occurrences are observed in the western Arctic, over the Chucki and the Canadian seas. The influence of the ground type is also investigated. Results show clearly that MPC and MPC-IB are more frequent over ocean than over land, particularly in winter and spring over the Svalbard region and during autumn over the whole Arctic and western regions.

ACPD
14, 23453–23497, 2014

Finally, we show that the spatial and vertical variability of MPC-IB is very similar to the one found for MPC. MPC-IB represent between 55 and 70 % of MPC over the whole Artic and between 65 and 80 % over the Svalbard region. However, MPC-IB statistics must be used with caution as the measurement uncertainties linked to the discrimination of multilayer MPC from single-layer MPC based on CALIPSO-CloudSat observations remains difficult to assess. Moreover, only few previous studies tried to quantify the multilayer cloud occurrence. For example, Verlinde et al. (2013) and Intrieri et al. (2002) show that multi-layers clouds may be as frequent as single-layer clouds. Our results show that single layer MPC are slightly more frequent than multilayer MPC (with a ratio varying between 55 and 80 % to the benefit of MPC-IB).

The present study allows for a quantification of the spatial and vertical occurrence of Arctic MPC at regional scale. Results highlight that Arctic, and particularly the Svalbard area, is a very favorable region for the formation and evolution of MPC and MPC-IB. However, all processes controlling MPC life cycle remain difficult to understand. Indeed, these processes are numerous and occur at different spatial and temporal scales, leading to complex interactions between them (Morrison et al., 2012). Furthermore, Arctic region benefits from peculiar meteorological conditions (Orbaek et al., 1999) and large-scale atmospheric circulation patterns.

The larger MPC and MPC-IB occurrences observed over the Svalbard compared to the averaged Arctic may be linked to the contribution of the humid air and warmer water transported from the North-Atlantic Ocean. This specific synoptic regime brings to the Svalbard region (and region of Greenland sea) more moisture compared to the rest of the Arctic (Serreze and Barry, 2005). Thus the cloud formation and their development can be amplified, since the moisture amount brought from North Atlantic is a source for initiation of liquid droplets and thus participates to the maintaining of equilibrium between ice and supercooled water. This leads to a larger occurrence of mixed phase in this region. Moreover, winter and transition seasons are known for their frequent stable atmospheric conditions (Orbaek et al., 1999). These conditions, associated with temperature and eventually with humidity inversions at cloud top frequently occurring in these seasons (Nygård et al., 2014; Sedlar et al., 2012), can contribute to the persistence of Arctic clouds and MPC at low altitudes by preventing formation of mixed phase at higher altitude levels. So, it is likely that boundary layer clouds presence is enhanced during these periods. Summer and fall seasons exhibit large occurrence values for MPC in western Arctic (Chucki and Canadian seas, Fig. 3a). During these seasons, the large open water allows to a part of warm water to be transported across the Arctic, resulting in warm and moist air advected in the western Arctic. Open water facilitates the vertical transfer of moisture, responsible of more clouds formation than over sea ice, which could explain the prevalence of MPC during this period in western Arctic.

So, this study highlights that sea ice melting and large-scale circulation can have an important impact on MPC annual variability in Arctic, by preventing warm water and moisture advection to the whole Arctic during winter and early spring, and promoting it the rest of the year (which is consistent with Kay and Gettelman, 2009; Palm et al., 2010).The decrease of low-level clouds and MPC in summer could be explained by an increase in air temperature coupled with less stable atmospheric conditions than during the rest of the year, promoting the formation of MPC at higher altitudes (as shown on vertical profiles in Figs. 4a and 6a).

Finally, it is obvious that numerous other regional and local processes are involved in the MPC life cycle and exert an influence on their spatial and temporal variability. Further studies are needed to investigate these different processes and establish a link between them. For example, many efforts are currently focused on the study of local sources or long-range transported aerosols in the Arctic region and their role acting as cloud condensation nuclei (CCN) or ice nuclei (IN). Such works, as those made by Avramov et al. (2011), Jackson et al. (2012) or Tjernström et al. (2014), will allow to better understand the liquid and ice phase formation within Arctic MPC. Otherwise, Orellana et al. (2011) and Tjernström et al. (2014) recent works highlight that sea ice melting during summer produces biogenic aerosol particles which could potentially act as CCN or IN for cloud and MPC formation. The influence of the surface, the turbulence and dynamics effects at small and large temporal and spatial scales on MPC occurrence needs also to be assessed. The most difficult task remains to couple all these processes and quantify their respective importance in Arctic MPC evolution.

6 Conclusions and outlook

This work presents a study of clouds and mixed phase clouds occurrence over the Arctic region with a focus on the Svalbard region. The methodology used is based on satellite active remote sensing measurements. The CALIPSO/CLOUDSAT observations are processed with the DARDAR retrieval algorithm to perform a cloud thermodynamic phase classification.

The study presents first a comparison of the various previous works investigating cloud occurrence in the Arctic from active remote sensing. Results from the main ground observatories are showed highlighting large differences in cloud variability from one observation site to another or from one instrumentation to another. This result leads to the conclusion that clouds climatologies made from ground site observatories are not completely representative of the whole Arctic. Their generalization to the regional scale has to be done with care. It is thus essential to use in addition a uniform observation technic to measure clouds over the whole Arctic, such as satellite observations.

Results from CALIPSO/CLOUDSAT observations show that clouds are ubiquitous in the Arctic throughout the year, with occurrence between 50 and nearly 100 %, depending on the season and the location. Moreover, clouds are more frequent in the Svalbard region than in the mean Arctic by around 5–10 %.

Then, mixed phase clouds (MPC) have been studied. The main results show that MPC occurrence over the whole Arctic is 30 % in winter and around 50 % the rest of the year. Over the Svalbard region, MPC occurrence is larger and more constant all along the year, with values around 55 %. Spatial and vertical MPC variability have been studied, as well as the influence of surface type on the MPC occurrence. MPC are

Discussion Paper | Discussion Paper | Discussion Paper | Discussion Paper |

ACPD

14, 23453–23497, 2014

Variability of the mixed phase in the Arctic with a focus on the Svalbard region

G. Mioche et al.

mainly present at low-altitudes since between 70 and 90 % of MPC are located below 3 km (both for the whole Arctic and the Svalbard region), especially in winter, spring and autumn. Summer presents a significant MPC occurrence at mid-level altitude domain (3–6 km). Low-level MPC annual variability presents a maximum of 45 % in spring and autumn for the whole Arctic. Over the Svalbard region, MPC occurrence is larger than the rest of the Arctic and rather constant throughout the year (55 %). Moreover, MPC are more frequently encountered over sea than over land, and this difference is more contrasted over the Svalbard.

Finally, we investigate the particular Arctic MPC consisting of a supercooled liquid top and ice in the lower part of the cloud (MPC-IB). This type of clouds represent between 55 and 70 % of the MPC over the whole Arctic and between 65 and 80 % of the MPC over the Svalbard region. Spatial, seasonal and vertical variability of this cloud type are studied and present strong similarities with MPC.

Differences between MPC seasonality over the Svalbard region and over the whole Arctic region are partially explained by the particular atmospheric conditions and the proximity of the North Atlantic Ocean encountered around the Svalbard. But strong similarities are also observed between MPC over the Arctic region and their counterparts in the rest of the Arctic. First, MPC have the same vertical distribution over the Svalbard region as over the whole Arctic, with prevalence of low-level clouds. Also, it is highlighted that MPC preferentially occur over ocean, both for the Svalbard region and the whole Arctic. At last, the large MPC amount observed in spring over Svalbard due to proximity of warm air and water from the North Atlantic Ocean seems to reproduce later in summer and fall in western Arctic when heat and moisture are the most present due to sea ice melting at that time.

MPC presence in the Arctic and their variability depend of the regional scale characteristics such as the oceanic circulation, and of more local conditions such as the proportion of open water/sea ice which exhibit a seasonal variability.

These results are based on satellite lidar and radar observations, and these instruments present some well-known shortcomings which may have a significant impact on

ACPD
14, 23453–23497, 2014

the present study. A part of this work focuses on these uncertainties. We investigate in particular the influence of the minimum altitude limit to take into account in order to avoid ground clutter contamination, showing that differences between a 500 m altitude threshold and 1000 m altitude threshold lie between 7 and 17 % depending on the cloud type and location. Active remote sensing must also be used with care when trying to discriminate multi-layer clouds from single-layer cloud due to the strong attenuation of lidar by supercooled liquid droplets, and thus its reduced capability to detect several superimposed supercooled liquid layers.

Since MPC over the Svalbard region and the rest of Arctic exhibit relatively similar occurrence properties, in-situ measurements performed over the Svalbard can be adequate to study Arctic MPC.

As an example, in situ airborne measurements performed during ASTAR 2007 campaign, in spring, over the Svalbard region, provided data from several boundary layer mixed phase clouds, with typical MPC-IB structure (Gayet et al., 2009). Several ascents and descents in all of these clouds have been performed between clouds top and the sea level. Despite the small amount of data collected and the fact that they are very localized in time and space, these in situ measurements can be considered as a well representative dataset for studying MPC at small scale.

Thereby, such in situ dataset will provide a more thorough characterization of MPC properties at small scale, and so by extension to typical MPC occurring in the Arctic. Such a study will provide in particular the quantification of ice and liquid particles microphysical and optical properties, vertical profiles of water droplets and ice crystals microphysical properties, giving an insight of microphysical processes responsible of particles growth within MPC. Accurate profiles of relevant clouds parameters (for example asymmetry parameter, optical depth, ice/liquid water mass fraction, ice crystals morphology, size and concentration, among others) may also be provided to contribute to the improvement of cloud representation in global and mesoscale models and to improve airborne and spatial remote sensing retrieval algorithms such as those of CALIPSO/CloudSat or in the near future EarthCare.

Finally, it would be of great interest to associate the present work with further studies at various scales, especially at small scale. The synergy of in situ and remote sensing observations will allow the study of MPC at multi-scale and it will particularly help to resolve some actual unanswered questions concerning the definition of mixed phase according to the scale of observation. Such a multi-scale approach will thus improve the parameterization of MPC in remote sensing retrieval algorithm and their representation in model at different resolutions.

Acknowledgements. This work is part of the french scientific community EECLAT project (Expecting EarthCare, Learning from A-Train) and is supported by the french Centre National des Etudes Spatiales (CNES). This research used resources from ICARE center for space remote sensing data processing.

References

Avramov, A., Ackerman, A. S., Fridlind, A. M., van Diedenhoven, B., Botta, G., Aydin, K., Verlinde, J., Korolev, A. V., Strapp, J. W., McFarquhar, G. M., Jackson, R., Brooks, S. D., Glen, A., and Wolde, M.: Toward ice formation closure in Arctic mixed-phase boundary layer clouds during ISDAC, J. Geophys. Res., 116, D00T08, doi:10.1029/2011JD015910, 2011.

Baumgardner, D., Avallone, L., Bansemer, A., Borrmann, S., Brown, P., Bundke, U., Chuang, P. Y., Cziczo, D., Field, P., Gallagher, M., Gayet, J.-F., Heymsfield, A., Korolev, A., Krämer, M., McFarquhar, G., Mertes, S., Möhler, O., Lance, S., Lawson, P., Petters, M. D., Pratt, K., Roberts, G., Rogers, D., Stetzer, O., Stith, J., Strapp, W., Twohy, C., and Wendisch, M.: In situ, airborne instrumentation: addressing and solving measurement problems in ice clouds, B. Am. Meteorol. Soc., 93, ES29–ES34, doi:10.1175/BAMS-D-11-00123.1, 2012.

Benedetti, A.: CloudSat AN-ECMWF Ancillary Data Interface Control Document, Technical Document, CloudSat Data Process. Cent., Fort Collins, Colorado, 16 July,, 2005.

Bergeron, T.: On the physics of clouds and precipitation, Int. Union Geod. Geophys., 156–178, 1935.

Bierwirth, E., Ehrlich, A., Wendisch, M., Gayet, J.-F., Gourbeyre, C., Dupuy, R., Herber, A., Neuber, R., and Lampert, A.: Optical thickness and effective radius of Arctic boundary-layer clouds retrieved from airborne nadir and imaging spectrometry, Atmos. Meas. Tech., 6, 1189–1200, doi:10.5194/amt-6-1189-2013, 2013.

Blanchard, Y., Pelon, J., Eloranta, E. W., Moran, K. P., Delanoë, J., and Sèze, G.: A synergistic analysis of cloud cover and vertical distribution from A-Train and ground-based sensors over the high Arctic station EUREKA from 2006 to 2010, J. Appl. Meteorol. Clim., submitted, 2014.

De Boer, G., Eloranta, E. W., and Shupe, M. D.: Arctic mixed-phase stratiform cloud properties from multiple years of surface-based measurements at two high-latitude locations, J. Atmos. Sci., 66, 2874–2887, doi:10.1175/2009JAS3029.1, 2009.

De Boer, G., Chapman, W., Kay, J. E., Medeiros, B., Shupe, M. D., Vavrus, S., and Walsh, J.: A characterization of the present-day arctic atmosphere in CCSM4, J. Climate, 25, 2676–2695, doi:10.1175/JCLI-D-11-00228.1, 2012.

Ceccaldi, M., Delanoë, J., Hogan, R. J., Pounder, N. L., Protat, A., and Pelon, J.: From CloudSat-CALIPSO to EarthCare: evolution of the DARDAR cloud classification and its comparison to airborne radar-lidar observations, J. Geophys. Res.-Atmos., 118, 1–20, doi:10.1002/jgrd.50579, 2013.

Cesana, G., Kay, J. E., Chepfer, H., English, J. M., and de Boer, G.: Ubiquitous low-level liquid-containing Arctic clouds: new observations and climate model constraints from CALIPSO-GOCCP, Geophys. Res. Lett., 39, L20804, doi:10.1029/2012GL053385, 2012.

Chan, M. A. and Comiso, J. C.: Arctic cloud characteristics as derived from MODIS, CALIPSO, and CloudSat, J. Climate, 26, 3285–3306, doi:10.1175/JCLI-D-12-00204.1, 2013.

Chernokulsky, A. and Mokhov, I. I.: Climatology of total cloudiness in the Arctic: an intercomparison of observations and reanalyses, Adv. Meteorol., 2012, 542093, doi:10.1155/2012/542093, 2012.

Choi, Y.-S., Ho, C.-H., Park, C.-E., Storelvmo, T., and Tan, I.: Influence of cloud phase composition on climate feedbacks, J. Geophys. Res.-Atmos., 119, 3687–3700, doi:10.1002/2013JD020582, 2014.

Curry, J. A.: Interactions among aerosols, clouds, and climate of the Arctic Ocean, Sci. Total Environ., 160–161, 777–791, doi:10.1016/0048-9697(95)04411-S, 1995.

Curry, J. A., Schramm, J. L., Rossow, W. B., and Randall, D.: Overview of Arctic cloud and radiation characteristics, J. Climate, 9, 1731–1764, doi:10.1175/1520-0442(1996)009<1731:OOACAR>2.0.CO;2, 1996.

Curry, J. A., Pinto, J. O., Benner, T., and Tschudi, M.: Evolution of the cloudy boundary layer during the autumnal freezing of the Beaufort Sea, J. Geophys. Res., 102, 13851, doi:10.1029/96JD03089, 1997.

Curry, J. A., Hobbs, P. V., King, M. D., Randall, D. A., Minnis, P., Isaac, G. A., Pinto, J. O., Uttal, T., Bucholtz, A., Cripe, D. G., Gerber, H., Fairall, C. W., Garrett, T. J., Hudson, J., Intrieri, J. M., Jakob, C., Jensen, T., Lawson, P., Marcotte, D., Nguyen, L., Pilewskie, P., Rangno, A., Rogers, D. C., Strawbridge, K. B., Valero, F. P. J., Williams, A. G., and Wylie, D.: FIRE Arctic Clouds Experiment, B. Am. Meteorol. Soc., 81, 5–29, doi:10.1175/1520-0477(2000)081<0005:FACE>2.3.CO;2, 2000.

Delanoë, J. and Hogan, R. J.: A variational scheme for retrieving ice cloud properties from combined radar, lidar, and infrared radiometer, J. Geophys. Res., 113, D07204, doi:10.1029/2007JD009000, 2008.

Delanoë, J. and Hogan, R. J.: Combined CloudSat-CALIPSO-MODIS retrievals of the properties of ice clouds, J. Geophys. Res., 115, D0029, doi:10.1029/2009JD012346, 2010.

Delanoë, J., Protat, A., Jourdan, O., Pelon, J., Papazzoni, M., Dupuy, R., Gayet, J.-F., and Jouan, C.: Comparison of airborne in situ, airborne radar-lidar, and spaceborne radar-lidar retrievals of polar ice cloud properties sampled during the POLARCAT Campaign, J. Atmos. Ocean. Tech., 30, 57–73, doi:10.1175/JTECH-D-11-00200.1, 2013.

Dong, X., Xi, B., Crosby, K., Long, C. N., Stone, R. S., and Shupe, M. D.: A 10 year climatology of Arctic cloud fraction and radiative forcing at Barrow, Alaska, J. Geophys. Res., 115, D17212, doi:10.1029/2009JD013489, 2010.

Ehrlich, A., Wendisch, M., Bierwirth, E., Gayet, J.-F., Mioche, G., Lampert, A., and Mayer, B.: Evidence of ice crystals at cloud top of Arctic boundary-layer mixed-phase clouds derived from airborne remote sensing, Atmos. Chem. Phys., 9, 9401–9416, doi:10.5194/acp-9-9401-2009, 2009.

Findeisen, W.: Kolloid-meteorologische Vorgänge bei Niederschlagsbildung, Meteorol. Z., 55, 121–133, 1938.

Frey, R. A., Ackerman, S. A., Liu, Y., Strabala, K. I., Zhang, H., Key, J. R., and Wang, X.: Cloud Detection with MODIS, Part I: Improvements in the MODIS Cloud Mask for Collection 5, J. Atmos. Ocean. Tech., 25, 1057–1072, doi:10.1175/2008JTECHA1052.1, 2008.

Garrett, T. J., Maestas, M. M., Krueger, S. K., and Schmidt, C. T.: Acceleration by aerosol of a radiative-thermodynamic cloud feedback influencing Arctic surface warming, Geophys. Res. Lett., 36, L19804, doi:10.1029/2009GL040195, 2009.

ACPD
14, 23453–23497, 2014

Variability of the mixed phase in the Arctic with a focus on the Svalbard region

G. Mioche et al.

Title Page
Abstract | Introduction
Conclusions | References
Tables | Figures
◀| |▶
◀ ▶
Back | Close
Full Screen / Esc
Printer-friendly Version
Interactive Discussion

Gayet, J.-F., Mioche, G., Dörnbrack, A., Ehrlich, A., Lampert, A., and Wendisch, M.: Microphysical and optical properties of Arctic mixed-phase clouds. The 9 April 2007 case study., Atmos. Chem. Phys., 9, 6581–6595, doi:10.5194/acp-9-6581-2009, 2009.
Harrington, J. Y., Reisin, T., Cotton, W. R., and Kreidenweis, S. M.: Cloud resolving simulations of Arctic stratus, Atmos. Res., 51, 45–75, doi:10.1016/S0169-8095(98)00098-2, 1999.
Hobbs, P. V. and Rangno, A. L.: Microstructures of low and middle-level clouds over the Beaufort Sea, Q. J. Roy. Meteor. Soc., 124, 2035–2071, doi:10.1002/qj.49712455012, 1998.
Huang, Y., Siems, S. T., Manton, M. J., Protat, A., and Delanoë, J.: A study on the low-altitude clouds over the Southern Ocean using the DARDAR-MASK, J. Geophys. Res.-Atmos., 117, D18204, doi:10.1029/2012JD017800, 2012.
Intrieri, J. M., Shupe, M. D., Uttal, T., and McCarty, B. J.: An annual cycle of Arctic cloud characteristics observed by radar and lidar at SHEBA, J. Geophys. Res., 107, doi:10.1029/2000JC000423, 2002.
Jackson, R. C., McFarquhar, G. M., Korolev, A. V., Earle, M. E., Liu, P. S. K., Lawson, R. P., Brooks, S., Wolde, M., Laskin, A., and Freer, M.: The dependence of ice microphysics on aerosol concentration in arctic mixed-phase stratus clouds during ISDAC and M-PACE, J. Geophys. Res., 117, D15207, doi:10.1029/2012JD017668, 2012.
Jouan, C., Girard, E., Pelon, J., Gultepe, I., Delanoë, J., and Blanchet, J.-P.: Characterization of Arctic ice cloud properties observed during ISDAC, J. Geophys. Res., 117, D23207, doi:10.1029/2012JD017889, 2012.
Jouan, C., Pelon, J., Girard, E., Ancellet, G., Blanchet, J. P., and Delanoë, J.: On the relationship between Arctic ice clouds and polluted air masses over the North Slope of Alaska in April 2008, Atmos. Chem. Phys., 14, 1205–1224, doi:10.5194/acp-14-1205-2014, 2014.
Jourdan, O., Mioche, G., Garrett, T. J., Schwarzenböck, A., Vidot, J., Xie, Y., Shcherbakov, V., Yang, P., and Gayet, J.-F.: Coupling of the microphysical and optical properties of an Arctic nimbostratus cloud during the ASTAR 2004 experiment: implications for light-scattering modeling, J. Geophys. Res., 115, D23206, doi:10.1029/2010JD014016, 2010.
Kay, J. E. and Gettelman, A.: Cloud influence on and response to seasonal Arctic sea ice loss, J. Geophys. Res., 114, D18204, doi:10.1029/2009JD011773, 2009.
Key, J. and Barry, R. G.: Cloud cover analysis with Arctic AVHRR data: 1. Cloud detection, J. Geophys. Res., 94, 18521, doi:10.1029/JD094iD15p18521, 1989.
Klein, S. A., McCoy, R. B., Morrison, H., Ackerman, A. S., Avramov, A., Boer, G. de, Chen, M., Cole, J. N. S., Del Genio, A. D., Falk, M., Foster, M. J., Fridlind, A., Golaz, J.-C., Hashino, T.,

ACPD
14, 23453–23497, 2014

Harrington, J. Y., Hoose, C., Khairoutdinov, M. F., Larson, V. E., Liu, X., Luo, Y., McFarquhar, G. M., Menon, S., Neggers, R. A. J., Park, S., Poellot, M. R., Schmidt, J. M., Sednev, I., Shipway, B. J., Shupe, M. D., Spangenberg, D. A., Sud, Y. C., Turner, D. D., Veron, D. E., Salzen, K. von, Walker, G. K., Wang, Z., Wolf, A. B., Xie, S., Xu, K.-M., Yang, F., and Zhang, G.: Intercomparison of model simulations of mixed-phase clouds observed during the ARM Mixed-Phase Arctic Cloud Experiment, I: Single-layer cloud, Q. J. Roy. Meteor. Soc., 135, 979–1002, doi:10.1002/qj.416, 2009.

Komurcu, M., Storelvmo, T., Tan, I., Lohmann, U., Yun, Y., Penner, J. E., Wang, Y., Liu, X., and Takemura, T.: INter-comparison of the cloud water phase among global climate models: cloud water phase in GCMs, J. Geophys. Res.-Atmos., 119, 3372–3400, doi:10.1002/2013JD021119, 2014.

Korolev, A. and Isaac, G.: Phase transformation of mixed-phase clouds, Q. J. Roy. Meteor. Soc., 129, 19–38, doi:10.1256/qj.01.203, 2003.

Liu, Y., Ackerman, S. A., Maddux, B. C., Key, J. R., and Frey, R. A.: Errors in cloud detection over the Arctic using a satellite imager and implications for observing feedback mechanisms, J. Climate, 23, 1894–1907, doi:10.1175/2009JCLI3386.1, 2010.

Liu, Y., Key, J. R., Ackerman, S. A., Mace, G. G., and Zhang, Q.: Arctic cloud macrophysical characteristics from CloudSat and CALIPSO, Remote Sens. Environ., 124, 159–173, doi:10.1016/j.rse.2012.05.006, 2012.

Luo, Y., Xu, K.-M., Morrison, H., McFarquhar, G. M., Wang, Z., and Zhang, G.: Multi-layer arctic mixed-phase clouds simulated by a cloud-resolving model: comparison with ARM observations and sensitivity experiments, J. Geophys. Res., 113, D12208, doi:10.1029/2007JD009563, 2008.

Marchand, R., Mace, G. G., Ackerman, T., and Stephens, G.: Hydrometeor detection using cloudsat – an Earth–Orbiting 94 GHz Cloud Radar, J. Atmos. Ocean. Tech., 25, 519–533, doi:10.1175/2007JTECHA1006.1, 2008.

McFarquhar, G. M., Zhang, G., Poellot, M. R., Kok, G. L., McCoy, R., Tooman, T., Fridlind, A., and Heymsfield, A. J.: Ice properties of single-layer stratocumulus during the Mixed-Phase Arctic Cloud Experiment: 1. Observations, J. Geophys. Res., 112, D24201, doi:10.1029/2007JD008633, 2007.

McFarquhar, G. M., Ghan, S., Verlinde, J., Korolev, A., Strapp, J. W., Schmid, B., Tomlinson, J. M., Wolde, M., Brooks, S. D., Cziczo, D., Dubey, M. K., Fan, J., Flynn, C., Gultepe, I., Hubbe, J., Gilles, M. K., Laskin, A., Lawson, P., Leaitch, W. R., Liu, P., Liu, X., Lubin, D.,

ACPD
14, 23453–23497, 2014

Variability of the mixed phase in the Arctic with a focus on the Svalbard region

G. Mioche et al.

Mazzoleni, C., Macdonald, A.-M., Moffet, R. C., Morrison, H., Ovchinnikov, M., Shupe, M. D., Turner, D. D., Xie, S., Zelenyuk, A., Bae, K., Freer, M., and Glen, A.: Indirect and semi-direct aerosol campaign: the impact of Arctic aerosols on clouds, B. Am. Meteorol. Soc., 92, 183–201, doi:10.1175/2010BAMS2935.1, 2011.

Morrison, H., McCoy, R. B., Klein, S. A., Xie, S., Luo, Y., Avramov, A., Chen, M., Cole, J. N. S., Falk, M., Foster, M. J., Del Genio, A. D., Harrington, J. Y., Hoose, C., Khairoutdinov, M. F., Larson, V. E., Liu, X., McFarquhar, G. M., Poellot, M. R., von Salzen, K., Shipway, B. J., Shupe, M. D., Sud, Y. C., Turner, D. D., Veron, D. E., Walker, G. K., Wang, Z., Wolf, A. B., Xu, K.-M., Yang, F., and Zhang, G.: Intercomparison of model simulations of mixed-phase clouds observed during the ARM Mixed-Phase Arctic Cloud Experiment, II: Multilayer cloud, Q. J. Roy. Meteor. Soc., 135, 1003–1019, doi:10.1002/qj.415, 2009.

Morrison, H., de Boer, G., Feingold, G., Harrington, J., Shupe, M. D., and Sulia, K.: Resilience of persistent Arctic mixed-phase clouds, Nat. Geosci., 5, 11–17, doi:10.1038/ngeo1332, 2012.

Nygård, T., Valkonen, T., and Vihma, T.: Characteristics of Arctic low-tropospheric humidity inversions based on radio soundings, Atmos. Chem. Phys., 14, 1959–1971, doi:10.5194/acp-14-1959-2014, 2014.

Orbaek, J. B., Hisdal, V., and Svaasand, L. E.: Radiation climate variability in Svalbard: surface and satellite observations, Polar Res., 18, 127–134, 1999.

Orellana, M. V., Matrai, P. A., Leck, C., Rauschenberg, C. D., Lee, A. M., and Coz, E.: Marine microgels as a source of cloud condensation nuclei in the high Arctic, P. Natl. Acad. Sci. USA, 108, 13612–13617, doi:10.1073/pnas.1102457108, 2011.

Palm, S. P., Strey, S. T., Spinhirne, J., and Markus, T.: Influence of Arctic sea ice extent on polar cloud fraction and vertical structure and implications for regional climate, J. Geophys. Res., 115, D21209, doi:10.1029/2010JD013900, 2010.

Rossow, W. B. and Garder, L. C.: Cloud detection using satellite measurements of infrared and visible radiances for ISCCP, J. Climate, 6, 2341–2369, doi:10.1175/1520-0442(1993)006<2341:CDUSMO>2.0.CO;2, 1993.

Sanderson, M. G., Hemming, D. L., and Betts, R. A.: Regional temperature and precipitation changes under high-end (= 4 °C) global warming, Philos. T. Roy. Soc. A, 369, 85–98, doi:10.1098/rsta.2010.0283, 2011.

Schweiger, A. J. and Key, J. R.: Arctic cloudiness: comparison of ISCCP-C2 and Nimbus-7 satellite-derived cloud products with a surface-based cloud climatology, J. Climate, 5, 1514–1527, doi:10.1175/1520-0442(1992)005<1514:ACCOIC>2.0.CO;2, 1992.

ACPD
14, 23453–23497, 2014

Sedlar, J., Shupe, M. D., and Tjernström, M.: On the relationship between thermodynamic structure and cloud top, and its climate significance in the Arctic, J. Climate, 25, 2374–2393, doi:10.1175/JCLI-D-11-00186.1, 2012.

Serreze, M. C. and Barry, R. G.: The Arctic Climate System, Cambridge University Press, Cambridge, UK, 2005.

Serreze, M. C., Barrett, A. P., Stroeve, J. C., Kindig, D. N., and Holland, M. M.: The emergence of surface-based Arctic amplification, The Cryosphere, 3, 11–19, doi:10.5194/tc-3-11-2009, 2009.

Shupe, M. D.: Clouds at Arctic Atmospheric Observatories, Part II: thermodynamic phase characteristics, J. Appl. Meteorol. Clim., 50, 645–661, doi:10.1175/2010JAMC2468.1, 2011.

Shupe, M. D. and Intrieri, J. M.: Cloud Radiative Forcing of the Arctic Surface: The Influence of Cloud Properties, Surface Albedo, and Solar Zenith Angle, J. Climate, 17, 616–628, doi:10.1175/1520-0442(2004)017<0616:crfota>2.0.co;2, 2004.

Shupe, M. D., Uttal, T., and Matrosov, S. Y.: Arctic cloud microphysics retrievals from surface-based remote sensors at SHEBA, J. Appl. Meteorol., 44, 1544–1562, doi:10.1175/JAM2297.1, 2005.

Shupe, M. D., Matrosov, S. Y., and Uttal, T.: Arctic mixed-phase cloud properties derived from surface-based sensors at SHEBA, J. Atmos. Sci., 63, 697–711, doi:10.1175/JAS3659.1, 2006.

Shupe, M. D., Walden, V. P., Eloranta, E., Uttal, T., Campbell, J. R., Starkweather, S. M., and Shiobara, M.: Clouds at Arctic Atmospheric Observatories, Part I: occurrence and macrophysical properties, J. Appl. Meteorol. Clim., 50, 626–644, doi:10.1175/2010JAMC2467.1, 2011.

Solomon, S., Qin, D., Manning, M., Chen, Z., Marquis, M., Averyt, K. B., Tignor, M., and Miller, H. L.: Climate Change 2007: The Physical Scence Basis, Cambridge University Press, Cambridge, UK, 2007.

Stephens, G. L.: Cloud feedbacks in the climate system: a critical review, J. Climate, 18, 237–273, 2005.

Stephens, G. L., Vane, D. G., Boain, R. J., Mace, G. G., Sassen, K., Wang, Z., Illingworth, A. J., O'Connor, E. J., Rossow, W. B., Durden, S. L., Miller, S. D., Austin, R. T., Benedetti, A., Mitrescu, C., and CloudSat Science Team: The CloudSat mission and the A-Train: a new dimension of space-based observations of clouds and precipitation, B. Am. Meteorol. Soc., 83, 1771–1790, doi:10.1175/BAMS-83-12-1771, 2002.

ACPD
14, 23453–23497, 2014

Thomas, S. M., Heidinger, A. K., and Pavolonis, M. J.: Comparison of NOAA's operational AVHRR-derived cloud amount to other satellite-derived cloud climatologies, J. Climate, 17, 4805–4822, 2004.

Tjernström, M., Leck, C., Birch, C. E., Bottenheim, J. W., Brooks, B. J., Brooks, I. M., Bäcklin, L., Chang, R. Y.-W., de Leeuw, G., Di Liberto, L., de la Rosa, S., Granath, E., Graus, M., Hansel, A., Heintzenberg, J., Held, A., Hind, A., Johnston, P., Knulst, J., Martin, M., Matrai, P. A., Mauritsen, T., Müller, M., Norris, S. J., Orellana, M. V., Orsini, D. A., Paatero, J., Persson, P. O. G., Gao, Q., Rauschenberg, C., Ristovski, Z., Sedlar, J., Shupe, M. D., Sierau, B., Sirevaag, A., Sjogren, S., Stetzer, O., Swietlicki, E., Szczodrak, M., Vaattovaara, P., Wahlberg, N., Westberg, M., and Wheeler, C. R.: The Arctic Summer Cloud Ocean Study (ASCOS): overview and experimental design, Atmos. Chem. Phys., 14, 2823–2869, doi:10.5194/acp-14-2823-2014, 2014.

Uttal, T., Curry, J. A., Mcphee, M. G., Perovich, D. K., Moritz, R. E., Maslanik, J. A., Guest, P. S., Stern, H. L., Moore, J. A., Turenne, R., Heiberg, A., Serreze, M. C., Wylie, D. P., Persson, O. G., Paulson, C. A., Halle, C., Morison, J. H., Wheeler, P. A., Makshtas, A., Welch, H., Shupe, M. D., Intrieri, J. M., Stamnes, K., Lindsey, R. W., Pinkel, R., Pegau, W. S., Stanton, T. P., and Grenfeld, T. C.: Surface heat budget of the Arctic Ocean, B. Am. Meteorol. Soc., 83, 255–275, doi:10.1175/1520-0477(2002)083<0255:SHBOTA>2.3.CO;2, 2002.

Verlinde, J., Harrington, J. Y., Yannuzzi, V. T., Avramov, A., Greenberg, S., Richardson, S. J., Bahrmann, C. P., McFarquhar, G. M., Zhang, G., Johnson, N., Poellot, M. R., Mather, J. H., Turner, D. D., Eloranta, E. W., Tobin, D. C., Holz, R., Zak, B. D., Ivey, M. D., Prenni, A. J., DeMott, P. J., Daniel, J. S., Kok, G. L., Sassen, K., Spangenberg, D., Minnis, P., Tooman, T. P., Shupe, M., Heymsfield, A. J., and Schofield, R.: The Mixed-Phase Arctic Cloud Experiment, B. Am. Meteorol. Soc., 88, 205–221, doi:10.1175/BAMS-88-2-205, 2007.

Verlinde, J., Rambukkange, M. P., Clothiaux, E. E., McFarquhar, G. M., and Eloranta, E. W.: Arctic multilayered, mixed-phase cloud processes revealed in millimeter-wave cloud radar Doppler spectra, J. Geophys. Res.-Atmos., 118, 13199–13213, doi:10.1002/2013JD020183, 2013.

Wang, X. and Key, J. R.: Arctic surface, cloud, and radiation properties based on the AVHRR Polar Pathfinder Dataset, Part I: spatial and temporal characteristics, J. Climate, 18, 2558–2574, doi:10.1175/JCLI3438.1, 2005.

Wegener, A.: Thermodynamik der Atmosphare, J. A. Barth, Leipzig, 1911.

Wielicki, B. A., Barkstrom, B. R., Harrison, E. F., Lee, R. B., Louis Smith, G., and Cooper, J. E.: Clouds and the Earth's Radiant Energy System (CERES): an earth observing system experiment, B. Am. Meteorol. Soc., 77, 853–868, doi:10.1175/1520-0477(1996)077<0853:CATERE>2.0.CO;2, 1996.

Winker, D. M., Pelon, J. R., and McCormick, M. P.: The CALIPSO Mission: Spaceborne Lidar for Observation of Aerosols and Clouds, Proceedings of SPIE, 4893, Hangzhou, China, 1–11, 2003.

Zygmuntowska, M., Mauritsen, T., Quaas, J., and Kaleschke, L.: Arctic Clouds and Surface Radiation – a critical comparison of satellite retrievals and the ERA-Interim reanalysis, Atmos. Chem. Phys., 12, 6667–6677, doi:10.5194/acp-12-6667-2012, 2012.

ACPD

14, 23453–23497, 2014

Table 1. DARDAR classes used in V1 version.

Class number	Definition
−9	Unknown
−1	Surface and subsurface
0	Clear sky
1	Ice only
2	Ice + supercooled water
3	Warm liquid
4	Supercooled water only
5	Rain or drizzle
6	Aerosols
7	Possibly insects
8	Stratospheric features

ACPD
14, 23453–23497, 2014

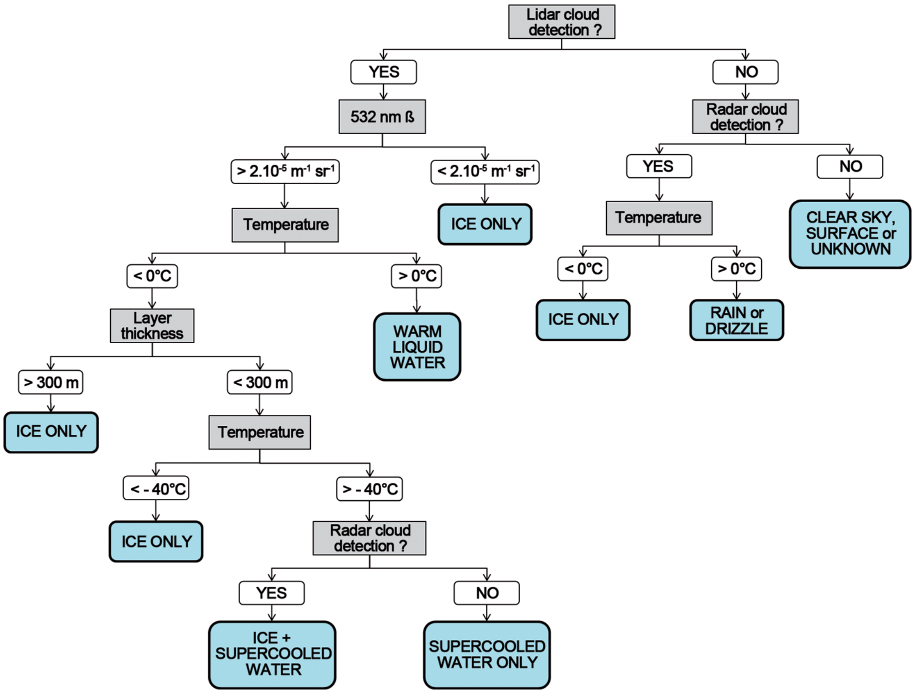

Figure 1. Representation of the DARDAR algorithm retrieval steps for cloud thermodynamic phase.

ACPD
14, 23453–23497, 2014

Variability of the mixed phase in the Arctic with a focus on the Svalbard region

G. Mioche et al.

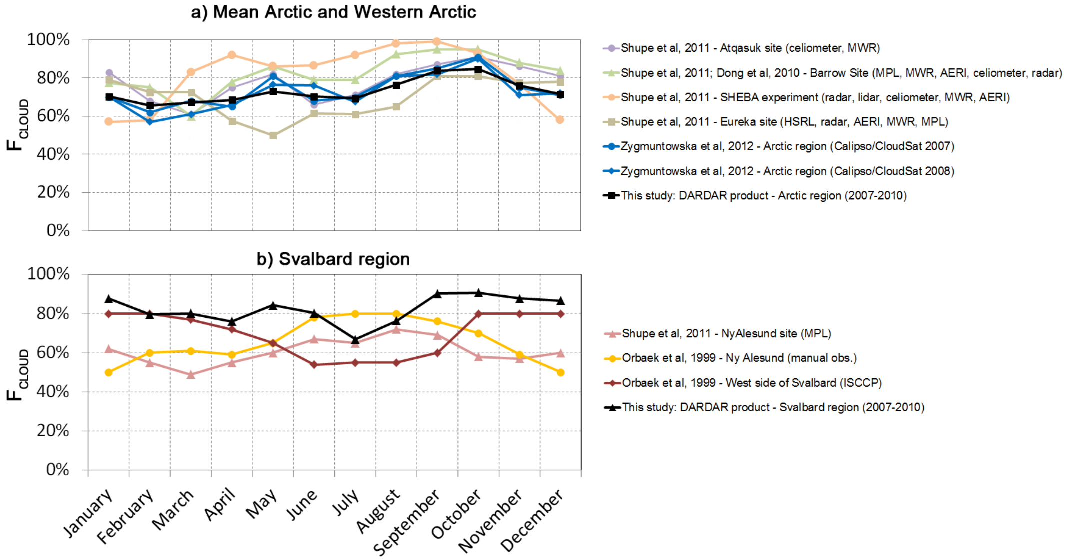

Figure 2. Monthly total cloud occurrence in Arctic from ground and spaceborne remote sensing observations: **(a)** over the whole Arctic region and western Arctic ground based sites; **(b)** over the Svalbard region.

ACPD
14, 23453–23497, 2014

Variability of the mixed phase in the Arctic with a focus on the Svalbard region

G. Mioche et al.

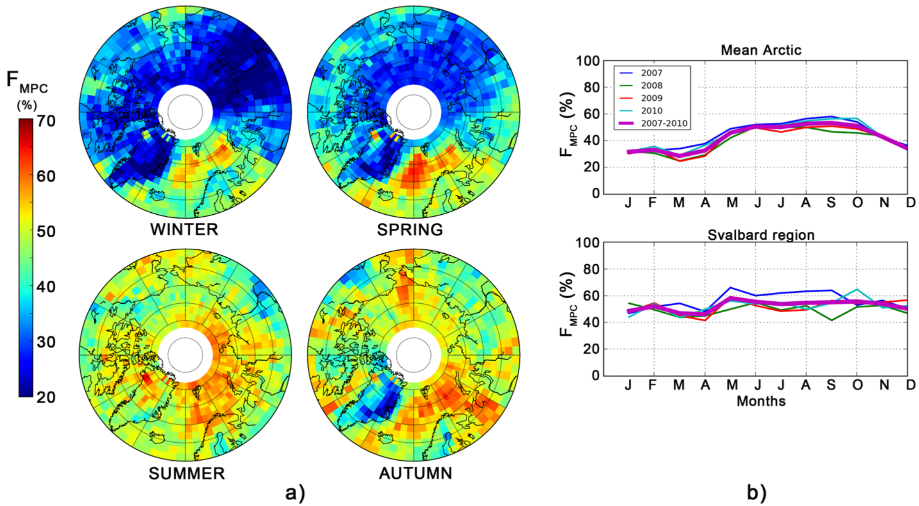

Figure 3. (a) Stereographic projection of seasonal MPC occurrence and **(b)** monthly MPC occurrence over the whole Arctic (top panel) and over the Svalbard region (bottom panel). Occurrences are computed taking into account 500 to 12 000 m altitude range.

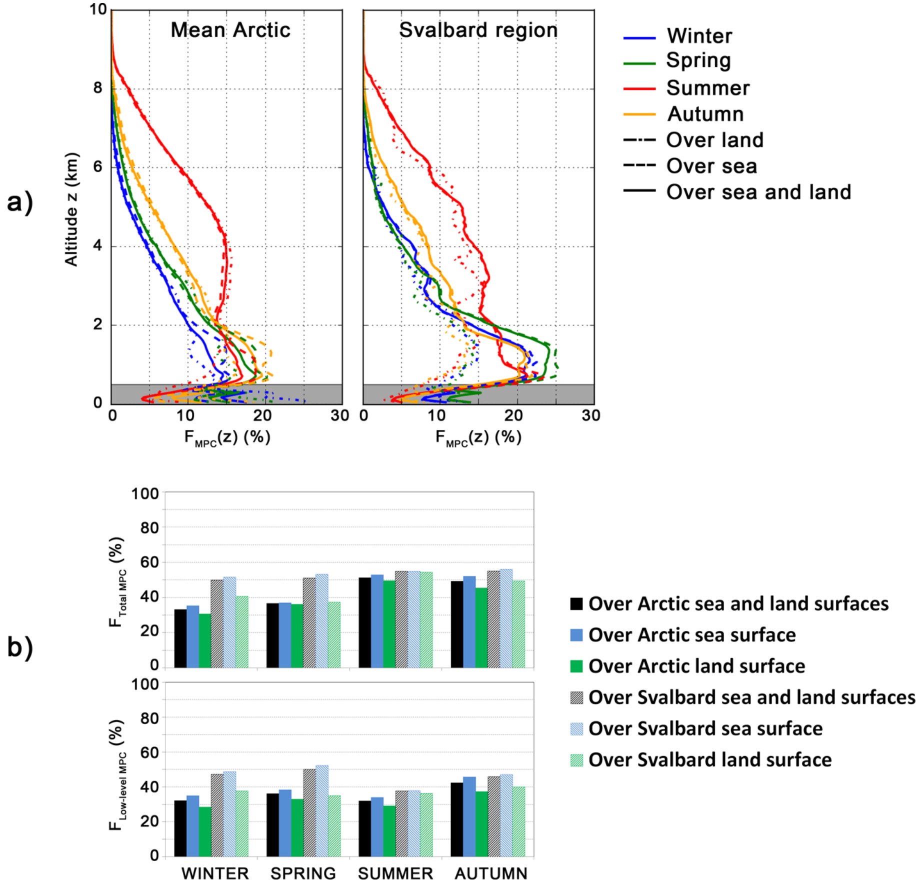

Figure 4. (a) Mean seasonal vertical profiles of MPC occurrence over the Arctic region (left panel) and over the Svalbard region (right panel); **(b)** mean seasonal MPC occurrence according to the surface type for all-level (500 m–12 km, top panel) and low-level (500 m–3 km, bottom panel) altitude domains.

ACPD
14, 23453–23497, 2014

Variability of the mixed phase in the Arctic with a focus on the Svalbard region

G. Mioche et al.

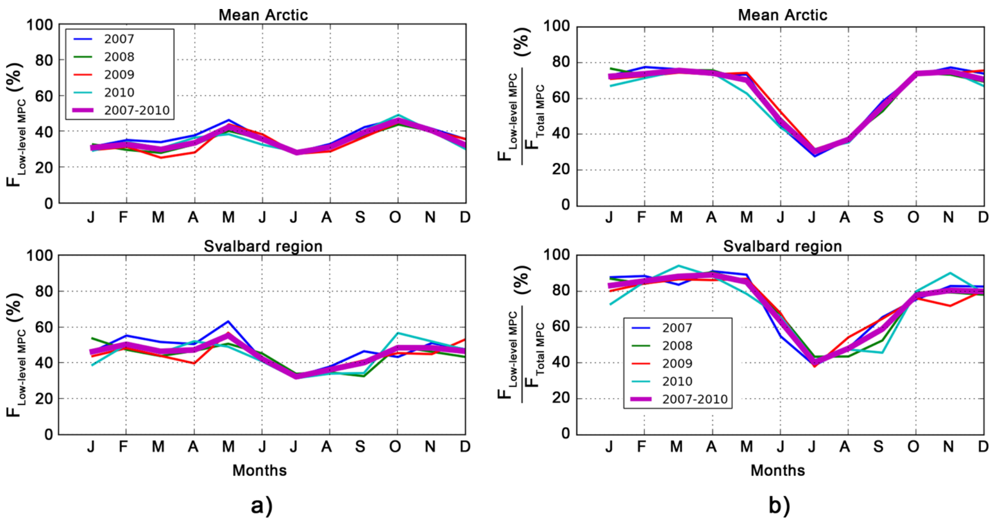

Figure 5. (a) Monthly low-level MPC occurrence and **(b)** ratio of low-level MPC over total MPC over the Arctic region (top panels) and over the Svalbard region (bottom panels).

ACPD
14, 23453–23497, 2014

Variability of the mixed phase in the Arctic with a focus on the Svalbard region

G. Mioche et al.

Title Page
Abstract Introduction
Conclusions References
Tables Figures
Back Close
Full Screen / Esc
Printer-friendly Version
Interactive Discussion

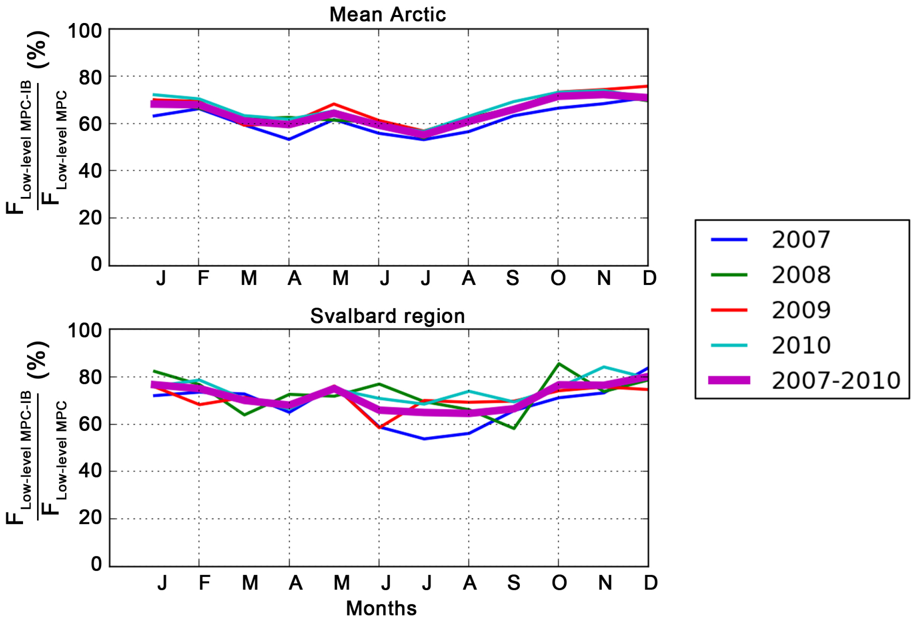

Figure 6. Monthly-averaged ratio of low-level MPC-IB over total MPC-IB over the Arctic region (top) and the Svalbard region (bottom).

ACPD
14, 23453–23497, 2014

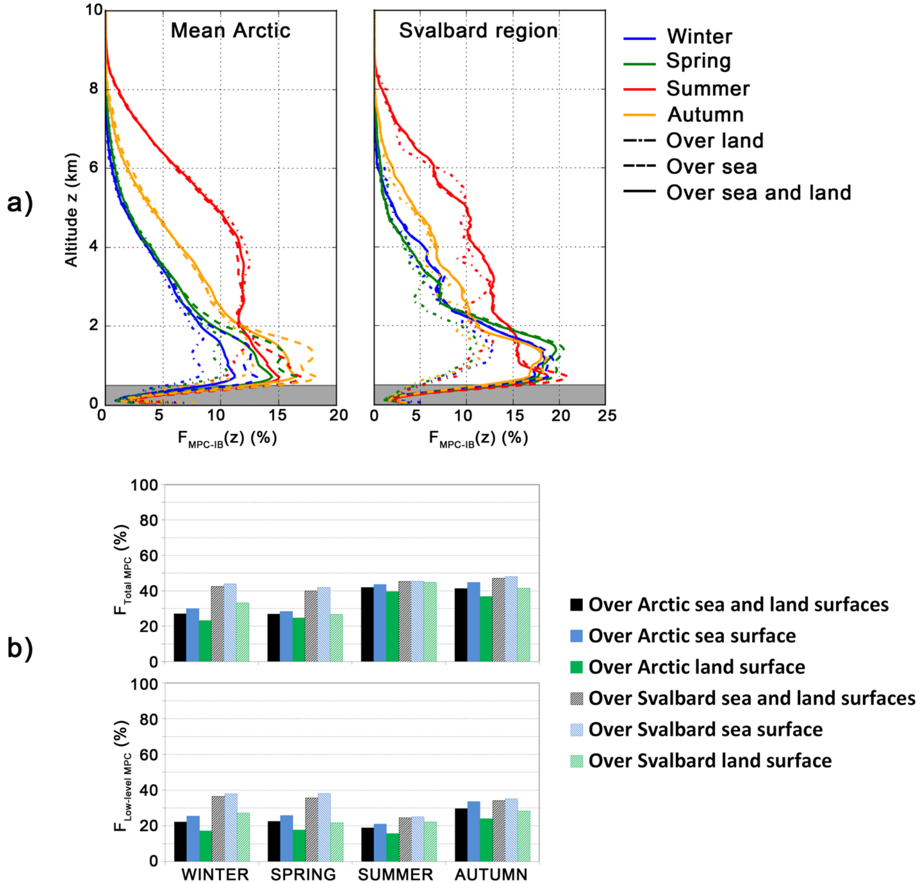

Figure 7. Same as Fig. 4 but for MPC-IB clouds.

ACPD
14, 23453–23497, 2014

Variability of the mixed phase in the Arctic with a focus on the Svalbard region

G. Mioche et al.

Title Page
Abstract | Introduction
Conclusions | References
Tables | Figures
◀ | ▶
Back | Close
Full Screen / Esc
Printer-friendly Version
Interactive Discussion

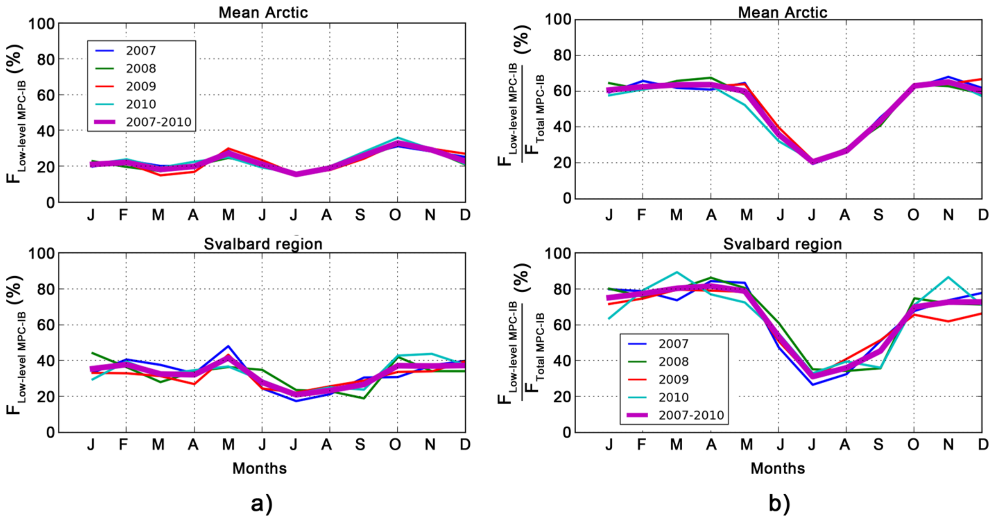

Figure 8. Same as Fig. 5 but for MPC-IB clouds.

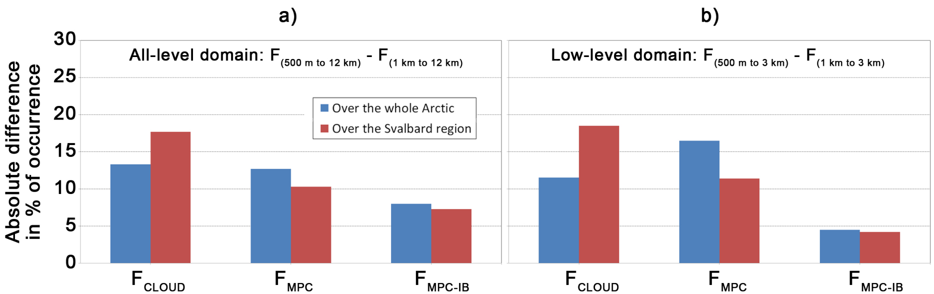

Figure 9. Absolute differences in % of occurrence between occurrences using a 1000 m altitude threshold and using a 500 m altitude threshold for total cloud, MPC and MPC-IB and for: **(a)** all-level and **(b)** low-level altitude domains.

ACPD
14, 23453–23497, 2014

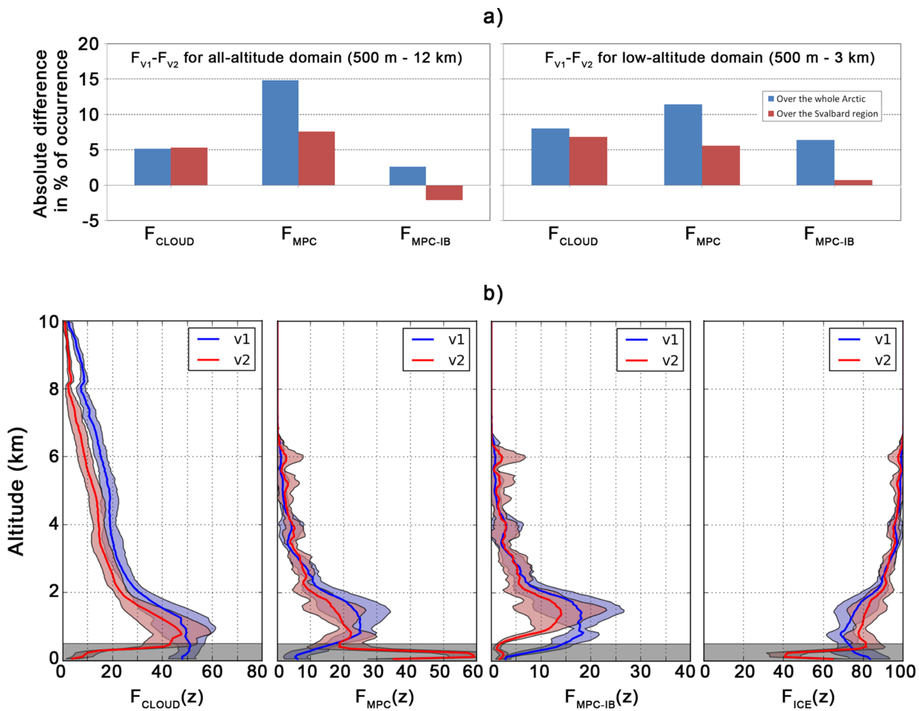

Figure 10. **(a)** Absolute differences in % of occurrence between occurrences computed from V1 and V2 DARDAR products for total cloud, MPC and MPC-IB and **(b)** mean vertical profiles of clouds, MPC, MPC-IB and ice clouds from V1 (blue lines) and V2 (red lines) DARDAR products for April 2007 over Svalbard. Filled areas represent standard deviation.

ACPD
14, 23453–23497, 2014